

10

Root Spaces and Dynkin Diagrams

Contents

10.1	Properties of Roots	179
10.2	Root Space Diagrams	181
10.3	Dynkin Diagrams	185
10.4	Conclusion	189
10.5	Problems	191

In the previous chapter the canonical commutation relations for semisimple Lie algebras were elegantly expressed in terms of roots. Although roots were introduced to simplify the expression of commutation relations, they can be used to classify Lie algebras and to provide a complete list of simple Lie algebras. We achieve both aims in this chapter. However, we use two different methods to accomplish this. We classify Lie algebras by specifying their root space diagrams. This is a relatively simple job using a 'building up' approach, adding roots to rank l root space diagrams to construct rank $l + 1$ root space diagrams. However, it is not easy to prove the completeness of root space diagrams by this method. Completeness is obtained by introducing Dynkin diagrams. These specify the inner products among a fundamental set of basis roots in the root space diagram. In this approach completeness is relatively simple to prove, while enumeration of the remaining roots within a root space diagram is less so.

10.1 Properties of Roots

In an effort to cast the commutation relations of a semisimple Lie algebra into an eigenvalue-eigenvector format, a secular equation was constructed from the regular representation. The rank of an algebra is, among other things:

- (i) The number of independent functions in the secular equation;
- (ii) The number of independent roots of the secular equation;
- (iii) The number of mutually commuting operators in the Lie algebra;

- (iv) The number of invariant operators that commute with all elements in the Lie algebra (Casimir operators);
- (v) The dimension of the positive-definite root space that summarizes the commutation relations.

In terms of the root space decomposition the commutation relations of the l (= rank) operators H_i and the shift operators E_α are

$$\begin{aligned}
 [H_i, H_j] &= 0 \\
 [\mathbf{H}, E_\alpha] &= \alpha E_\alpha \\
 [E_\alpha, E_\beta] &= \alpha \cdot \mathbf{H} && \alpha + \beta = 0 \\
 &= N_{\alpha, \beta} E_{\alpha + \beta} && \alpha + \beta \neq 0, \text{ a root} \\
 &= 0 && \alpha + \beta \text{ not a root}
 \end{aligned} \tag{10.1}$$

The coefficients $N_{\alpha, \beta}$ are defined in terms of the nonnegative integers m, n by

$$N_{\alpha, \beta + k\alpha}^2 = (n - k)(m + k + 1)(\alpha \cdot \alpha)/2 \tag{10.2}$$

where $\beta + k\alpha$ is a root only for $k = -m, \dots, +n$. The roots are normalized by

$$\sum_{\alpha \neq 0} \alpha \cdot \alpha = \text{rank} = l \tag{10.3}$$

In deriving the value for the structure constant $N_{\alpha, \beta}$ we observed

$$\begin{aligned}
 \frac{2(\alpha \cdot \beta)}{\alpha \cdot \alpha} &\quad \text{is an integer} \\
 \beta' = \beta - \frac{2(\alpha \cdot \beta)}{\alpha \cdot \alpha} \alpha &\quad \text{is a root}
 \end{aligned} \tag{10.4}$$

The root β' is obtained by reflecting β in the hyperplane orthogonal to α . These two observations are all that is required to construct root space diagrams of any rank.

If we write $2(\alpha \cdot \beta)/(\alpha \cdot \alpha) = n$ and $2(\alpha \cdot \beta)/(\beta \cdot \beta) = n'$, where n and n' are integers, then by the Schwartz inequality

$$0 \leq \cos^2(\alpha, \beta) = \left(\frac{\alpha \cdot \beta}{\alpha \cdot \alpha} \right) \left(\frac{\alpha \cdot \beta}{\beta \cdot \beta} \right) = \frac{n}{2} \frac{n'}{2} \leq 1 \tag{10.5}$$

These two results severely constrain the possible angles between two roots and their relative length. The results are summarized in Table 10.1.

Table 10.1. *Properties of roots in a root space diagram.*

$\cos^2(\alpha, \beta)$	$\theta(\alpha, \beta)$	$n = \frac{2\alpha \cdot \beta}{\alpha \cdot \alpha}$	$n' = \frac{2\alpha \cdot \beta}{\beta \cdot \beta}$	$\frac{\alpha \cdot \alpha}{\beta \cdot \beta} = \frac{n'}{n}$
1	$\frac{\pi}{2} \pm \frac{\pi}{2}$	± 2	± 2	1
$\frac{3}{4}$	$\frac{\pi}{2} \pm \frac{\pi}{3}$	± 3	± 1	3^{-1}
		± 1	± 3	3^{+1}
$\frac{2}{4}$	$\frac{\pi}{2} \pm \frac{\pi}{4}$	± 2	± 1	2^{-1}
		± 1	± 2	2^{+1}
$\frac{1}{4}$	$\frac{\pi}{2} \pm \frac{\pi}{6}$	± 1	± 1	1
0	$\frac{\pi}{2}$	0	0	-

10.2 Root Space Diagrams

The procedure for constructing root space diagrams in spaces of any dimension (= rank) is simple. Begin with the rank-one root space. It is unique, with nonzero vectors $\pm \mathbf{e}_1$. To construct rank two root spaces, add a non-collinear vector to this root space in such a way that the constraints exhibited in Table 10.1 are obeyed, and complete the root space by reflections in hyperplanes orthogonal to all roots. Only a small number of rank-two root spaces can be constructed in this way. These are $A_2, B_2 = C_2, D_2$ and G_2 , and are shown in Fig. 9.6.

Rank-three root spaces are constructed from rank-2 root spaces by the same process. A non coplanar vector is added to a rank-two root space diagram subject to the condition that all requirements of Table 10.1 are satisfied. The resultant set of roots is completed by reflection in hyperplanes orthogonal to all roots. If any pair of roots in the completed diagram does not satisfy these conditions, the resulting diagram is not an allowed root space diagram. The allowed rank-3 root space diagrams are shown in Fig. 10.1.

This procedure is inductive. All rank- l root space diagrams are constructed in this way from rank- $(l - 1)$ root space diagrams. We find by this building-up process that there are four infinite series of root spaces with the following sets of roots:

$$\begin{array}{llll}
 A_{l-1} & +\mathbf{e}_i - \mathbf{e}_j & 1 \leq i \neq j \leq l & l - 1 \geq 1 \\
 D_l & \pm \mathbf{e}_i \pm \mathbf{e}_j & 1 \leq i \neq j \leq l & l > 3 \\
 B_l & \pm \mathbf{e}_i \pm \mathbf{e}_j, \pm \mathbf{e}_i & 1 \leq i \neq j \leq l & l > 2 \\
 C_l & \pm \mathbf{e}_i \pm \mathbf{e}_j, \pm 2\mathbf{e}_i & 1 \leq i \neq j \leq l & l > 1
 \end{array} \tag{10.6}$$

The subscript on the letter indicates the rank of the root space. It is easily seen that D_l is constructed by adding roots $\pm(\mathbf{e}_i + \mathbf{e}_j)$ to A_{l-1} ,

and B_l, C_l are constructed by adding roots $\pm \mathbf{e}_i, \pm 2\mathbf{e}_i$ to D_l . The root spaces A_{l-1}, D_l, B_l, C_l are all inequivalent with the following exceptions

$$\begin{aligned} A_1 &= B_1 = C_1 \\ B_2 &= C_2 \\ A_3 &= D_3 \end{aligned} \tag{10.7}$$

The root space D_2 is semisimple

$$D_2 = A_1 + A_1 \tag{10.8}$$

In addition to these four unending series there are five exceptional root spaces:

$$\begin{aligned} G_2 & \quad +\mathbf{e}_i - \mathbf{e}_j \\ & \quad \pm [(\mathbf{e}_i + \mathbf{e}_j) - 2\mathbf{e}_k] \qquad 1 \leq i \neq j \neq k \leq 3 \\ \\ F_4 & \quad \pm \mathbf{e}_i \pm \mathbf{e}_j \\ & \quad \pm 2\mathbf{e}_i \\ & \quad \pm \mathbf{e}_1 \pm \mathbf{e}_2 \pm \mathbf{e}_3 \pm \mathbf{e}_4 \qquad 1 \leq i \neq j \leq 4 \\ \\ E_6 & \quad \pm \mathbf{e}_i \pm \mathbf{e}_j \\ & \quad \frac{1}{2} (\underbrace{\pm \mathbf{e}_1 \pm \mathbf{e}_2 \pm \mathbf{e}_3 \pm \mathbf{e}_4 \pm \mathbf{e}_5}_{\text{even number of + signs}}) \pm \frac{\sqrt{3}}{4} \mathbf{e}_6 \qquad 1 \leq i \neq j \leq 5 \\ \\ E_7 & \quad \pm \mathbf{e}_i \pm \mathbf{e}_j \\ & \quad \frac{1}{2} (\underbrace{\pm \mathbf{e}_1 \pm \mathbf{e}_2 \pm \mathbf{e}_3 \pm \mathbf{e}_4 \pm \mathbf{e}_5 \pm \mathbf{e}_6}_{\text{even number of + signs}}) \pm \frac{\sqrt{2}}{4} \mathbf{e}_7 \qquad 1 \leq i \neq j \leq 6 \\ \\ E_8 & \quad \pm \mathbf{e}_i \pm \mathbf{e}_j \\ & \quad \frac{1}{2} (\underbrace{\pm \mathbf{e}_1 \pm \mathbf{e}_2 \pm \mathbf{e}_3 \pm \mathbf{e}_4 \pm \mathbf{e}_5 \pm \mathbf{e}_6 \pm \mathbf{e}_7 \pm \mathbf{e}_8}_{\text{even number of + signs}}) \qquad 1 \leq i \neq j \leq 8 \end{aligned} \tag{10.9}$$

The building up principle is summarized in Fig. 10.2. In this figure all root spaces are shown by rank. Arrows connect pairs related by the building up principle.

Remark 1: The following classical groups are associated with these

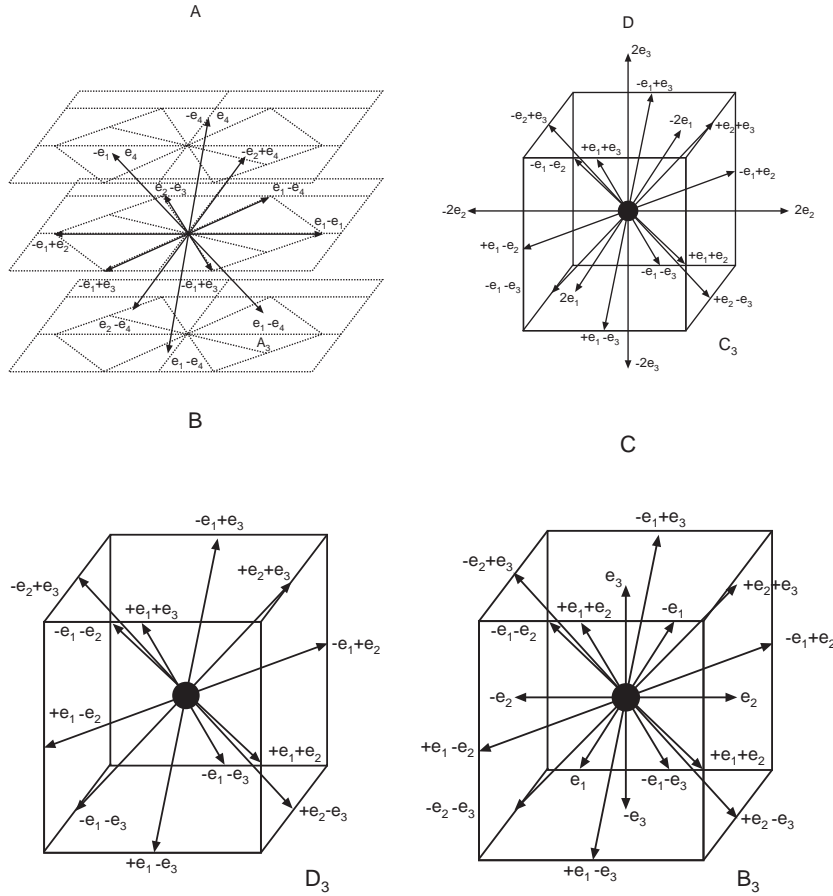


Fig. 10.1. Rank-3 root space diagrams. Top: A_3, D_3 . Bottom: B_3, C_3 .

root spaces

$$\begin{array}{llll}
 A_{l-1} & SU(l), SL(l; R), SU(p, q) & p + q = l & \\
 D_l & SO(2l), SO(p, q) & p + q = 2l & \\
 B_l & SO(2l + 1), SO(p, q) & p + q = 2l + 1 & (10.10) \\
 C_l & Sp(l), Sp(p, q) & p + q = l &
 \end{array}$$

Several different Lie groups (algebras) are associated with each root space. This comes about because root spaces classify complex Lie algebras. Recall that extension of the field from real to complex numbers was required to guarantee that the secular equation could be solved.

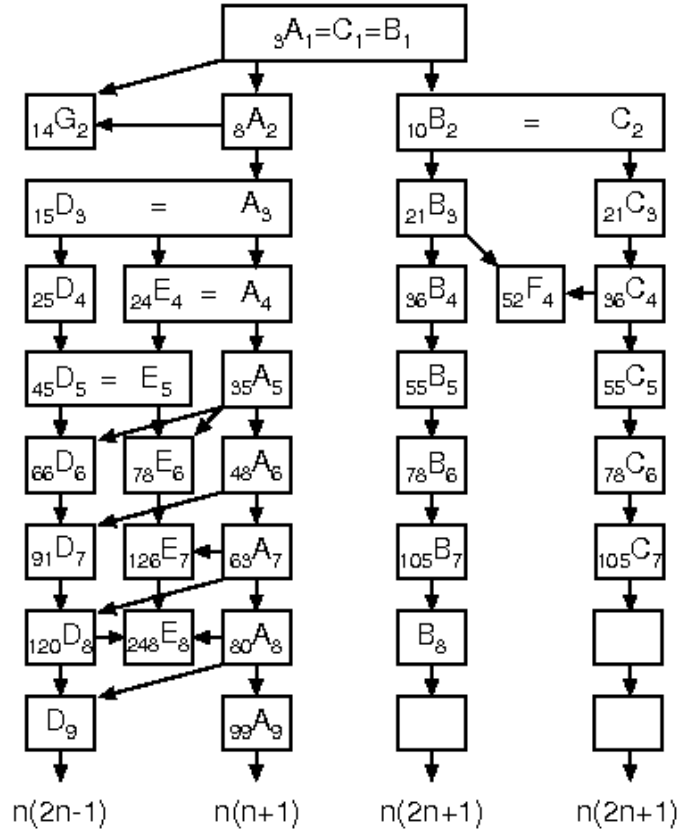


Fig. 10.2. Root spaces constructed by the building-up principle. There are four infinite series and five exceptional Lie algebras. The root spaces are organized by rank.

Each of the Lie algebras with the same root space has the same complex extension: for example, $SL(l; C)$ for A_{l-1} .

Remark 2: The root space D_2 consists of two orthogonal sets of roots $\pm(\mathbf{e}_1 - \mathbf{e}_2)$ and $\pm(\mathbf{e}_1 + \mathbf{e}_2)$. The decomposition is shown in Fig. 10.3. Orthogonal root spaces describe semisimple Lie algebras. Root subspaces that do not have an orthogonal decomposition describe simple Lie algebras. Complete reducibility of the regular representation corresponds to decomposition of the root space into disjoint (orthogonal) root spaces and of the semisimple Lie algebras to simple invariant subalgebras.

Remark 3: The root spaces B_2 and C_2 are equivalent, as is easily

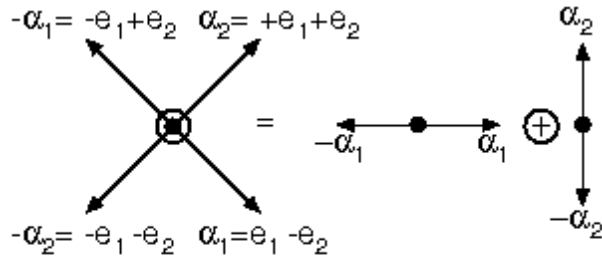


Fig. 10.3. The root space D_2 consists of two orthogonal root subspaces. Both describe the rank-one algebra A_1 .

seen by rotation. The root space B_2 describes $SO(5)$ while C_2 describes $Sp(2) = U(2; Q)$, which has a 4-dimensional matrix representation obtained by replacing each quaternion by a complex 2×2 matrix. Therefore we should expect $SO(5)$ to have a 4-dimensional ‘spinor’ representation based on $U(2; Q)$ in the same way that $SO(3)$ (B_1) has a 2-dimensional spinor representation based on $U(1; Q)$ or $SU(2)$ (A_1).

Remark 4: In the building-up construction the roots in each root space diagram are explicitly constructed. What is not immediately obvious is that there are no more simple root spaces than those listed. How are we sure that there are no more than five exceptional root spaces? This question is not easy to resolve in the context of root space constructions alone. However, it is easily resolved by another algorithmic procedure. This procedure easily yields a beautiful completeness argument. The price we pay is a somewhat greater difficulty in constructing the complete set of roots for these spaces. However, since they have been constructed above, this poses no severe limitation.

10.3 Dynkin Diagrams

A plane through the origin of a root space diagram that does not contain any nonzero roots divides the roots into two sets, one ‘positive,’ the other negative (cf. Figs. 9.6). Among the positive roots the l nearest to this hyperplane in a rank- l root space are linearly independent. They can therefore be chosen as a basis set in this space. These roots are called **fundamental roots**, and denoted $\alpha_1, \alpha_2, \dots, \alpha_l$. Every positive root can be expressed in terms of this basis as a linear combination

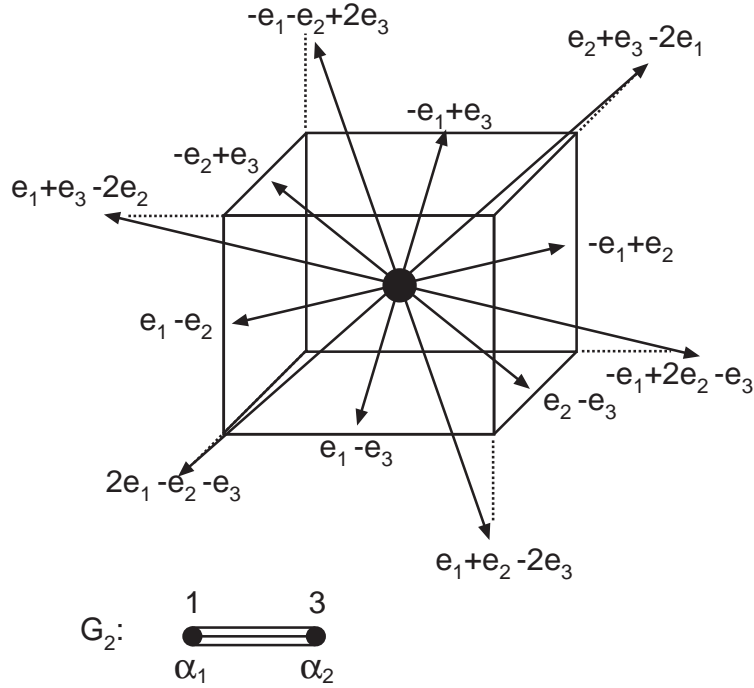


Fig. 10.4. Root space for G_2 . Fundamental roots are $\alpha_1 = \mathbf{e}_1 - \mathbf{e}_2$ and $\alpha_2 = -\mathbf{e}_1 + 2\mathbf{e}_2 - \mathbf{e}_3$. All roots are orthogonal to $\mathbf{R} = \mathbf{e}_1 + \mathbf{e}_2 + \mathbf{e}_3$.

of these fundamental roots with integer coefficients. The integers are all positive or zero, because every shift operator defined by a positive root can be written as a multiple commutator of shift operators with fundamental positive roots. By symmetry, every negative root is a linear combination of fundamental roots with nonpositive integer coefficients. The fundamental roots for G_2 are shown in Fig. 10.4. Fundamental roots for the root spaces A_{l-1}, D_l, B_l, C_l are

	α_1	α_2	α_3	\dots	α_{l-1}	α_l
$A_{l-1} :$	$\mathbf{e}_1 - \mathbf{e}_2$	$\mathbf{e}_2 - \mathbf{e}_3$	$\mathbf{e}_3 - \mathbf{e}_4$	\dots	$\mathbf{e}_{l-1} - \mathbf{e}_l$	
$D_l :$	"	"	"	\dots	"	$\mathbf{e}_{l-1} + \mathbf{e}_l$
$B_l :$	"	"	"	\dots	"	\mathbf{e}_l
$C_l :$	"	"	"	\dots	"	$2\mathbf{e}_l$

(10.11)

Inner products among the fundamental roots are summarized conveniently in a diagrammatic form. The inner product between two funda-

mental roots is negative or zero

$$(\alpha_i, \alpha_j) = -\sqrt{n_{ij}/4} \tag{10.12}$$

where n_{ij} is 0, 1, 2, or 3. Each fundamental root is represented by a dot. Dots i and j are joined by n_{ij} lines. Orthogonal roots are not connected. Such a diagram is called a **Dynkin diagram**. The Dynkin diagram for the semisimple Lie algebra represented by orthogonal root spaces $G_2 + B_3$ is shown in Fig. 10.5.

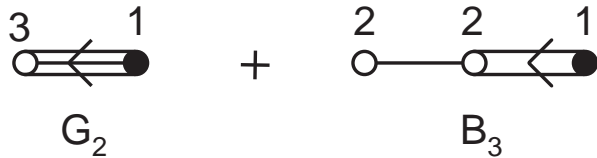


Fig. 10.5. Disconnected Dynkin diagrams describe simple Lie algebras. Here the disconnected diagram describes $G_2 \oplus B_3$.

Orthogonal root spaces for semisimple Lie algebras are represented by disconnected Dynkin diagrams. In these diagrams the relative (squared) lengths of the fundamental roots (3, 1 for G_2) are indicated over the root symbol, by an arrow pointing from the shorter to the longer, and by open and solid dots. The conventions are interchangeable: normally not more than one is adopted. We will use only one at a time.

Only a very limited number of distinct kinds of Dynkin diagrams can occur. The limitations derive from two observations:

Observation 1: The root space is positive definite.

Observation 2: If \mathbf{v}_i is an orthonormal system of vectors in the root space and \mathbf{u} is a unit vector, then the direction cosines $\mathbf{u} \cdot \mathbf{v}_i$ obey

$$\sum (\mathbf{u} \cdot \mathbf{v}_i)^2 \leq 1 \tag{10.13}$$

These two observations are now used to list a set of properties that constrain the allowed Dynkin diagrams ever more tightly.

Property 1: There are no loops. A diagram containing a loop has at least as many lines as vertices. With $\mathbf{u}_i = \alpha_i/|\alpha_i|$ the inner product

$$\left(\sum \mathbf{u}_i, \sum \mathbf{u}_j\right) = n + 2 \sum \sum \mathbf{u}_i \cdot \mathbf{u}_j \geq 0 \tag{10.14}$$

cannot be positive since $2\mathbf{u}_i \cdot \mathbf{u}_j \leq -1$ if α_i and α_j are connected.

Property 2: The number of lines connected to any node is less than four. This results from Observation 2. If \mathbf{v}_i are connected to \mathbf{u} , then

$$\sum (\mathbf{u} \cdot \mathbf{v}_i)^2 = \sum n_i/4 < 1 \tag{10.15}$$

Property 3: A simple chain connecting any two dots can be shrunk. An allowed diagram is transformed to an allowed diagram. This allows the construction shown in Fig. 10.6.

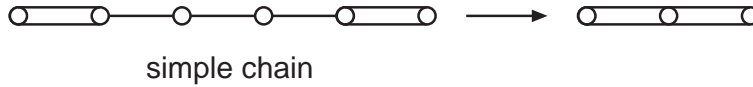


Fig. 10.6. A simple linear chain can be removed. If the original is an allowed Dynkin diagram, the shortened diagram is also an allowed Dynkin diagram. In this case the original diagram is not an allowed Dynkin diagram.

Since the constructed diagram violates Property 2, so also does the original diagram.

The only possibilities remaining are shown in Fig. 10.7.

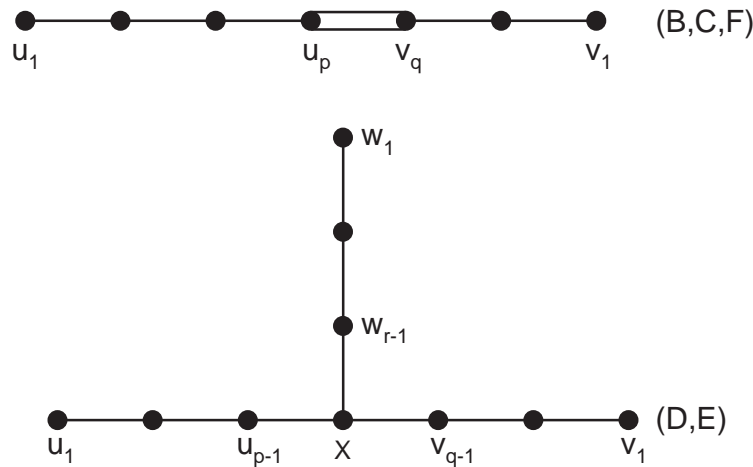


Fig. 10.7. General forms of allowed root space diagrams after the process of contraction has been performed.

For the diagrams (B, C, F) with a single double link, the Schwartz

inequality applied to the vectors

$$\mathbf{u} = \sum_{i=1}^p i \mathbf{u}_i \quad \mathbf{v} = \sum_{j=1}^q j \mathbf{v}_j \quad (10.16)$$

where $\mathbf{u}_i, \mathbf{v}_j$ are unit vectors $\mathbf{u}_i = \alpha_i/|\alpha_i|$ and $\mathbf{v}_i = \alpha_j/|\alpha_j|$, can be transformed to the inequality

$$\left(1 + \frac{1}{p}\right) \left(1 + \frac{1}{q}\right) > 2 \quad (10.17)$$

This has the following solutions with $p \geq q$

$$\begin{aligned} p \text{ arbitrary, } q = 1, & \quad B_l, C_l & \quad l = p + 1 \\ p = 2, \quad q = 2, & \quad F_4 \end{aligned} \quad (10.18)$$

For the diagrams (D, E) Observation 2 applied to the vectors \mathbf{u}, \mathbf{v} , and \mathbf{w} defined as in Eq. (10.16) leads to the inequality

$$\frac{1}{p} + \frac{1}{q} + \frac{1}{r} > 1 \quad (10.19)$$

This has the following solutions with $p \geq q \geq r \geq 2$

p	q	r	Root space
p	2	2	D_{p+2}
3	3	2	E_6
4	3	2	E_7
5	3	2	E_8

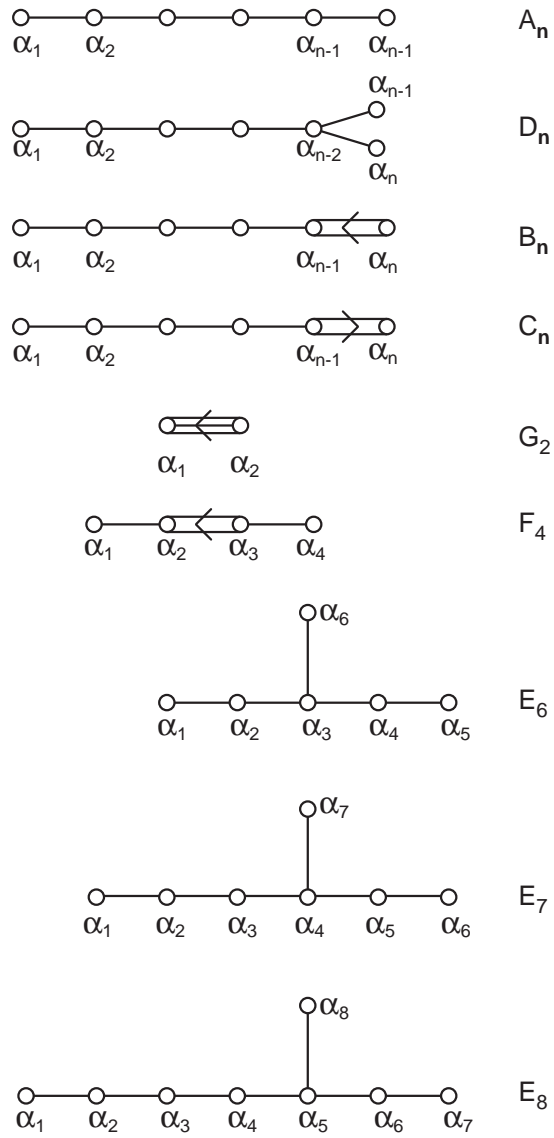
(10.20)

The allowed Dynkin diagrams are summarized in Table 10.2. This table provides a complete list of simple root spaces. Each root space has been constructed in Sec. 10.2. The complete set of roots in each of the root spaces is listed in that section.

10.4 Conclusion

The canonical commutation relations for a semisimple Lie algebra have been expressed in terms of root space diagrams. These diagrams have been used to classify all simple root space diagrams of rank l by constructing a complete set of roots inductively from each root space diagram of rank $l - 1$. The completeness of this construction is guaranteed by the 1:1 correspondence between the root space diagrams constructed in Sec. 10.2 and the allowed connected Dynkin diagrams constructed in Section 10.3

Table 10.2. Allowed root spaces.



10.5 Problems

1. Show that the following three statements for a semisimple Lie algebra are equivalent:

- a. The Lie algebra has two simple invariant subalgebras;
- b. The nonzero roots in its root space diagram fall into two mutually orthogonal subsets;
- c. Its Dynkin diagram is disconnected, with two connected components.

Do these statements extend to semisimple Lie algebras with three or more simple invariant subalgebras?

2. Show that bilinear combinations of two boson creation and/or annihilation operators can be identified with the roots in the 10-dimensional Lie algebra C_2 as shown in Fig. 10.8(a). Identify H_1 and H_2 .

3. Show that bilinear combinations of two fermion creation and/or annihilation operators can be identified with the roots in the 6-dimensional Lie algebra D_2 as shown in Fig. 10.8(b). Identify H_1 and H_2 .

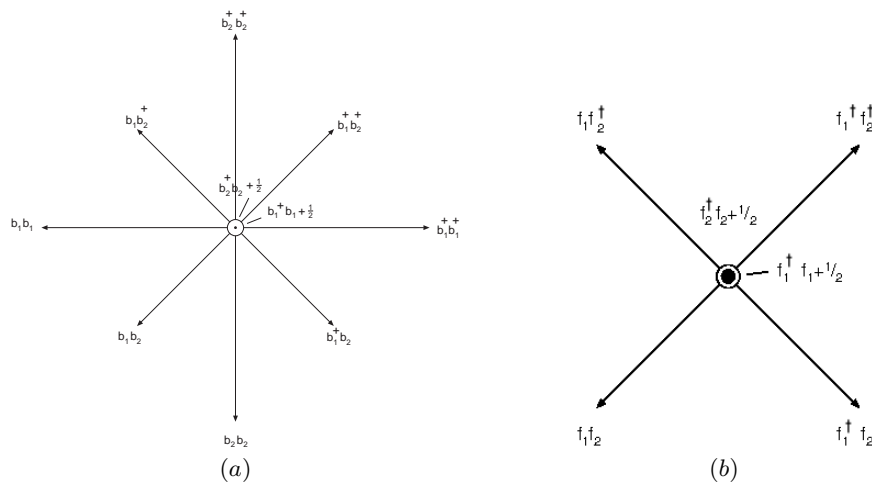


Fig. 10.8. (a) Roots of C_2 are identified with products of boson operators. (b) Roots of D_2 are identified with products of fermion operators. Note that $f_1^\dagger f_1^\dagger = 0$, etc.

4. Show that the following identifications are appropriate for the generators of the Lie group $U(l)$:

Canonical Form	Boson Operators	Coordinates & Derivatives	Fermion Operators
H_i	$b_i^\dagger b_i$	$x^i \partial_i$	$f_i^\dagger f_i$
$E_{+\mathbf{e}_i - \mathbf{e}_j}$	$b_i^\dagger b_j$	$x^i \partial_j$	$f_i^\dagger f_j$

5. Show that the following identifications are appropriate for the eigenoperators for the root spaces C_l and D_l :

C_l			D_l	
Canonical Form	Boson Operators	Coordinates & Derivatives	Fermion Operators	Coordinates & Derivatives
H_i	$b_i^\dagger b_i + \frac{1}{2}$	$x^i \partial_i$	$f_i^\dagger f_i + \frac{1}{2}$	$x^i \partial_i + \frac{1}{2}$
$E_{+\mathbf{e}_i - \mathbf{e}_j}$	$b_i^\dagger b_j$	$x^i \partial_j$	$f_i^\dagger f_j$	$x^i \partial_j$
$E_{+\mathbf{e}_i + \mathbf{e}_j}$	$b_i^\dagger b_j^\dagger$	$x^i x^j$	$f_i^\dagger f_j^\dagger$	$x^i x^j$
$E_{-\mathbf{e}_i - \mathbf{e}_j}$	$b_i b_j$	$\partial_i \partial_j$	$f_i f_j$	$\partial_i \partial_j$
$E_{+2\mathbf{e}_i}$	$b_i^\dagger b_i^\dagger$	$x^i x^i$		
$E_{-2\mathbf{e}_i}$	$b_i b_i$	$\partial_i \partial_i$		

6. Apply the Schwartz inequality to the two vectors in Eq. (10.16) and show that the result can be expressed in the form of the inequality given in Eq. (10.17).

7. Use the projection inequality of Eq. (10.13) with the three vectors constructed for the Dynkin diagrams of type (D, E) to obtain the inequality of Eq. (10.19).

8. A Lie algebra is spanned by n^2 operators of the form $a_i^\dagger a_j$, with $1 \leq i, j \leq n$. Show that the linear vector space for this algebra can be written as the direct sum of two subspaces: \mathbf{L}, \mathbf{Q} spanned by the operators

$$\begin{array}{ll}
 \mathbf{L} & \mathbf{Q} \\
 L_{ij} = a_i^\dagger a_j - a_j^\dagger a_i = -L_{ji} & Q_{ij} = a_i^\dagger a_j + a_j^\dagger a_i = +Q_{ji}
 \end{array}$$

For $n = 3$ the subspaces transform like an angular momentum vector and a quadrupole tensor. Show that the commutation relations are

$$\begin{array}{ll}
 [\mathbf{L}, \mathbf{L}] = \mathbf{L} & [L_{ij}, L_{rs}] = +\delta_{jr} L_{is} + \delta_{is} L_{jr} - \delta_{ir} L_{js} - \delta_{js} L_{ir} \\
 [\mathbf{L}, \mathbf{Q}] = \mathbf{Q} & [L_{ij}, Q_{rs}] = +\delta_{jr} Q_{is} - \delta_{is} Q_{jr} - \delta_{ir} Q_{js} + \delta_{js} Q_{ir} \\
 [\mathbf{Q}, \mathbf{Q}] = \mathbf{L} & [Q_{ij}, Q_{rs}] = +\delta_{jr} L_{is} + \delta_{is} L_{jr} + \delta_{ir} L_{js} + \delta_{js} L_{ir}
 \end{array}$$

The quadrupole tensor, in turn, with six components, can be written as the sum of a traceless tensor $\hat{\mathbf{Q}}$ and a scalar N :

$$\hat{N} = \sum_{i=1}^3 a_i^\dagger a_i \qquad \hat{Q}_{ij} = Q_{ij} - \frac{2}{3} \hat{N} \delta_{ij}$$

The operator \hat{N} commutes with all operators $a_i^\dagger a_j$. Interpret these commutation relations in physical terms (scalars, vectors and traceless quadrupole tensors) and in mathematical terms (commutative invariant subalgebra \hat{N} ; Cartan decomposition of a simple Lie algebra $\mathbf{L} + \hat{\mathbf{Q}}$).

9. Carry out a similar decomposition for any value of n . Show that the only changes in the discussion of Problem 8 are the dimensions of the spaces \mathbf{L} ($3 \rightarrow n(n-1)/2$), \mathbf{Q} ($6 \rightarrow n(n+1)/2$), and the definition of \hat{N} ($3 \rightarrow n$).